



**HAL**  
open science

# Catalytic Hydrogenation of Derived Vegetable Oils Using Ion-Exchange Resin-Supported Ruthenium Nanoparticles: Scope and Limitations

Antonio Madureira, Sébastien Noël, Bastien Léger, Anne Ponchel, Eric Monflier

► **To cite this version:**

Antonio Madureira, Sébastien Noël, Bastien Léger, Anne Ponchel, Eric Monflier. Catalytic Hydrogenation of Derived Vegetable Oils Using Ion-Exchange Resin-Supported Ruthenium Nanoparticles: Scope and Limitations. ACS Sustainable Chemistry & Engineering, 2022, 10 (50), pp.16588-16597. 10.1021/acssuschemeng.2c04178 . hal-03921924

**HAL Id: hal-03921924**

**<https://univ-artois.hal.science/hal-03921924v1>**

Submitted on 22 Nov 2023

**HAL** is a multi-disciplinary open access archive for the deposit and dissemination of scientific research documents, whether they are published or not. The documents may come from teaching and research institutions in France or abroad, or from public or private research centers.

L'archive ouverte pluridisciplinaire **HAL**, est destinée au dépôt et à la diffusion de documents scientifiques de niveau recherche, publiés ou non, émanant des établissements d'enseignement et de recherche français ou étrangers, des laboratoires publics ou privés.

# Catalytic hydrogenation of derived-vegetable oils using ion-exchange resin-supported ruthenium nanoparticles: scope and limitations

*Antonio Madureira, Sébastien Noël\*, Bastien Léger, Anne Ponchel and Eric Monflier*

Univ. Artois, CNRS, Centrale Lille, Univ. Lille, UMR 8181, Unité de Catalyse et Chimie du Solide (UCCS), rue Jean Souvraz, SP 18, 62300 Lens, France.

\*E-mail : [sebastien.noel@univ-artois.fr](mailto:sebastien.noel@univ-artois.fr)

**Keywords:** ion-exchange resin, vegetable oils, catalysis, ruthenium nanoparticles, hydrogenation.

**Abstract:** The hydrogenation of vegetable oils-derived compounds using ion-exchange resin-supported ruthenium nanoparticles was reported for the first time. These supported metal catalysts (Ru\_DOWEX<sub>2</sub>-X) were prepared by a simple two-step procedure using commercial and cheap materials and affording high efficiency with a low metal loading. They were characterized by several physicochemical techniques and showed well-dispersed ruthenium nanoparticles into robust beads of the strong cation-exchange resin DOWEX<sub>2</sub>-X. Their catalytic activity was evaluated in the hydrogenation of methyl undecenoate in heptane, under mild experimental conditions (30 °C, 10 bar of H<sub>2</sub>) and the high activities of the metal solid catalysts deeply depended on the water amount inside the pores. In terms of recyclability, several physicochemical analyses

after the successive catalytic runs showed the robustness of the immobilized ruthenium nanoparticles for which very low metal leaching and no particles aggregation were observed. The decrease of the catalytic activity could be explained by a progressive water loss contained in the resin pores which was illustrated by a decrease of the bead diameter. The immobilized ruthenium nanoparticles were also evaluated in the catalytic hydrogenation of vegetable oils and their corresponding methyl esters and showed a remarkable high activity compared to other catalytic systems tested under similar mild reaction conditions.

## **Introduction**

Nowadays, historically petro-based chemicals can be obtained from biomass resources such as cellulose, lignin or vegetable oils.<sup>1-3</sup> The increased demand for sustainable energy has attracted much interest for the development of alternative fuels that derived from traditional petroleum oil. Vegetable oils-derived compounds such as castor oil-based ricinoleic acid (12-hydroxy-9-octadecenoic acid) has been considered to be an important alternative to the diesel fuel.<sup>4-8</sup> Methyl undecenoate, which came from methyl ricinoleate pyrolysis, is also an interesting substrate because its carbon chain length is suitable for jet fuels.<sup>9</sup> The C=C hydrogenation of oleochemicals, one of the most encountered chemical transformations for these compounds, involved most of the cases metal heterogeneous catalysts.<sup>10-12</sup> For non-noble metal based-hydrogenation catalysts, nickel and copper have appeared to be good candidates.<sup>13-17</sup> Supported catalysts containing noble metals, e.g. rhodium,<sup>18</sup> palladium,<sup>19-21</sup> ruthenium,<sup>22-24</sup> and platinum<sup>25,26</sup> have also been investigated. According to our literature survey, the reaction conditions with supported metal catalysts are generally harsh in terms of temperature. For instance, Murzin's team studied the

hydrogenation of linoleic acid towards stearic acid in decane, in the presence of palladium or ruthenium-based catalysts at 100 °C under 20 bar of hydrogen.<sup>23</sup> The effects of a series of inorganic support materials on the catalytic performance of supported platinum catalysts for the soybean oil hydrogenation were evaluated under 5 bar at 140 °C.<sup>26</sup> Gallucci and coworkers performed the selective hydrogenation of canola and sunflower oils under different hydrogen pressures and temperatures with Lindlar catalyst (palladium on calcium carbonate, poisoned with lead).<sup>27</sup> The highest C18:1 amount was obtained under 4 bar of hydrogen at 180 °C.

Among the wide variety of metal nanoparticles (NPs) supports, ion-exchange resins (IER) show several advantages, including commercial availability, low cost, beneficial metal nanoparticles stabilization effects by both charged functional groups (electrostatic stabilization) and porosity (confinement effect and control of particles growth and aggregation) and easy recovery.<sup>28,29</sup> It is interesting to note that, when IER are swollen in the appropriate solvent, low-cross linked resins (typical 0.5 – 4 % cross-linkage) develop microporous gel structures with larger pores and higher porous volumes which are suitable for metal particles with diameters smaller than 10 nm.<sup>30,31</sup> Ion-exchange resin-supported metal nanoparticles could be used in a wide range of catalytic reactions including hydrogenation reactions.<sup>32–38</sup> For example, strong cation-exchange resins were used to immobilize palladium nanoparticles through a two-step procedure.<sup>36</sup> These materials were evaluated in the hydrogenation of a wide range of unsaturated compounds such as arenes, alkenes or alkynes under very mild conditions (room temperature, pressure inferior to 1 bar of hydrogen). The same authors developed the same strategy for the immobilization of rhodium NPs for the selective hydrogenation of substituted arenes. The acidic properties of the strong cation exchange resins were also used for the continuous production of  $\gamma$ -valerolactone using ruthenium NPs.<sup>38</sup> These catalysts where metal NPs grew within the pores of commercially insoluble polymers,

showed high activities while keeping their robustness. Surprisingly, no studies concerning their use in the hydrogenation of vegetable oils or the corresponding fatty acid methyl esters (FAMES) are referenced in the literature.

In this context, immobilized ruthenium nanoparticles on strong cation-exchange resins were synthesized in a two-step procedure by the immobilization of the Ru (III) cations followed by their reduction using sodium borohydride. In order to get a sufficient pore volume for the metal nanoparticles growth and for the diffusion of the oleochemicals inside the pores during the catalytic test, a 2 % cross-linkage was chosen. After optimizing the catalytic system with methyl undecenoate as the model substrate (beads size and water amount), the metal solid catalyst recycling was deeply studied to find the key parameters which could be controlled to keep its catalytic activity and its robustness. The supported ruthenium NPs were then evaluated towards the C=C hydrogenation of other oleochemicals such as FAMES and vegetable oils under mild reaction conditions.

## **Results and discussion**

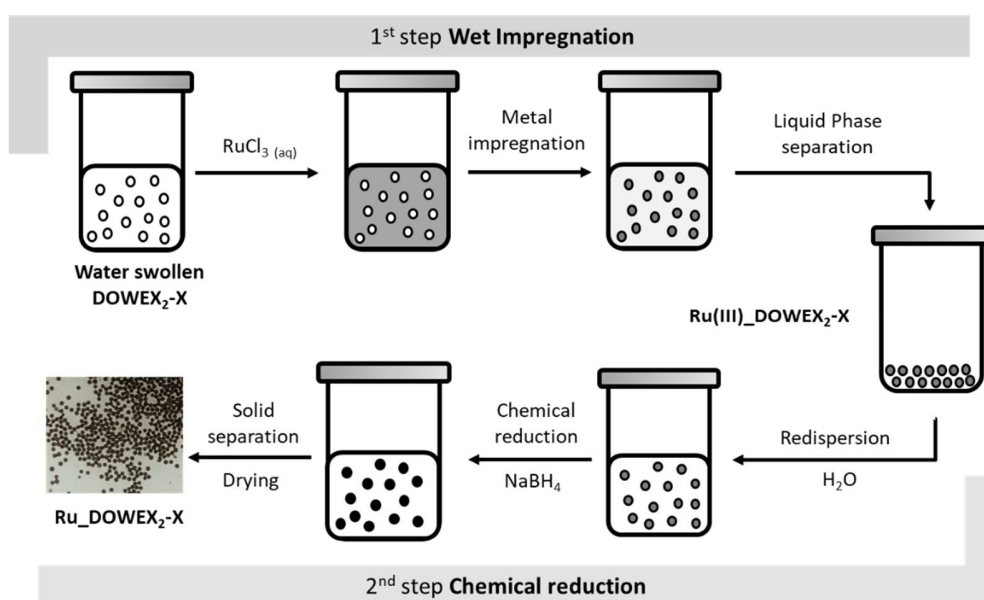
### **1. Synthesis and characterization of resin-supported ruthenium NPs**

Strong cation-exchange resins will be used in their parent sodium salt to stabilize Ru (III) species through electrostatic interactions. Taking into account the substrates which will be hydrogenated (vegetable oils and fatty acid methyl esters), these functionalized polystyrenes are crosslinked up to 2 % with divinylbenzene resulting in resins with high porous volumes ( $2.6 \text{ cm}^3 \cdot \text{g}^{-1}$ ).<sup>39</sup> Moreover, for a fixed cross-linkage, DOWEX® 50WX2-75 ( $\text{H}^+$  form, gel-type, 38-75  $\mu\text{m}$  bead size, 4.8 mequiv.  $\text{g}^{-1}$  exchange capacity) and DOWEX® 50WX2-300 ( $\text{H}^+$  form, gel-type, 150-300  $\mu\text{m}$  bead

size, 4.8 mequiv.  $\text{g}^{-1}$  exchange capacity) were used with the abbreviated notation (DOWEX<sub>2</sub>-75 and DOWEX<sub>2</sub>-300 respectively).

The procedure employed for the synthesis of ion-exchange resin-supported ruthenium nanoparticles is illustrated in **Scheme 1** and precisely described in ESI part. In a first step, the strong cation-exchange resin (*i.e.* containing sulfonic groups) was deprotonated into the parent sodium salt in order to improve the metalation of the resin but also to avoid the possible leaching of the further nanoparticles which can occur in the presence of acidic species. The amount of  $\text{H}^+$  exchanged with the cation  $\text{Na}^+$  was determined by an acid-basic titration of the aqueous supernatant with a hydrochloric acid solution. The obtained ratio of exchanged protons compared with the total amount of  $\text{H}^+$  present in the resin was 96%. The resins were then metalated in the presence of a ruthenium chloride solution (Ru(III)\_DOWEX<sub>2</sub>-X) and the supported ruthenium

**Scheme 1.** Sketch of ion-exchange resin-supported Ru NPs synthesis.



In the present study, the Ru-containing resins were characterized in solid state by several physicochemical techniques, after drying at 60 °C for 48 hours. The morphology of the resin beads was evaluated through scanning electron microscopy (SEM) experiments (**ESI-Figure S1**). The SEM images showed that the resin beads were not damaged by mechanical stirring and kept their spherical morphology with a bead diameter of  $61 \pm 11 \mu\text{m}$  for DOWEX<sub>2</sub>-75 and  $250 \pm 13 \mu\text{m}$  for DOWEX<sub>2</sub>-300. Neither the metalation nor reduction steps led to a beads cracking. The metal distribution was analysed by EDS elemental mapping and clearly showed that the ruthenium species were homogeneously distributed onto the support, indicating that water diffuses thoroughly into the beads during the metalation step.<sup>37,40</sup> EDS and ICP analyses led both to a ruthenium loading of 0.9 wt%. The efficiency of the incorporation of the ruthenium species is around 90 % (expected metal loading of 1 wt%) and could be explained by the high electrostatic interactions between the sulfonate groups and the Ru (III) ion.

Additional thermogravimetric experiments were carried out to evaluate the impact of the reduced ruthenium species on the thermal behavior of the resin. The TG profiles of natriated DOWEX<sub>2</sub>-X and Ru\_DOWEX<sub>2</sub>-X (X=75 and 300) carried out under nitrogen atmosphere are shown in **Figure 1**. The most distinct difference between the two thermal profiles is the adsorbed water amount within the resin (weight loss between 70 and 200°C), which is higher for DOWEX<sub>2</sub>-75. Moreover, this loss was less important in the case of the metalated resins (Ru\_DOWEX<sub>2</sub>-X) which could be explained by the presence of these ruthenium species which prevent the adsorption of water molecules inside the resin. A minor second weight loss (1-2 wt%), marked with a frame, was observed in the 340 - 470 °C range for the metalated resins but not in the case of natriated DOWEX<sub>2</sub>-X. This loss could be attributed to the anticipated decomposition of the polystyrene chains in the presence of metallic species.<sup>41</sup> A third weight loss occurred from 480 to 800°C and

could be linked to the polymeric chains cracking. No significant difference between the two samples was finally noticed. The TG profiles and the SEM images confirmed that the synthesis and the immobilization of the ruthenium nanoparticles did not damage the resin.

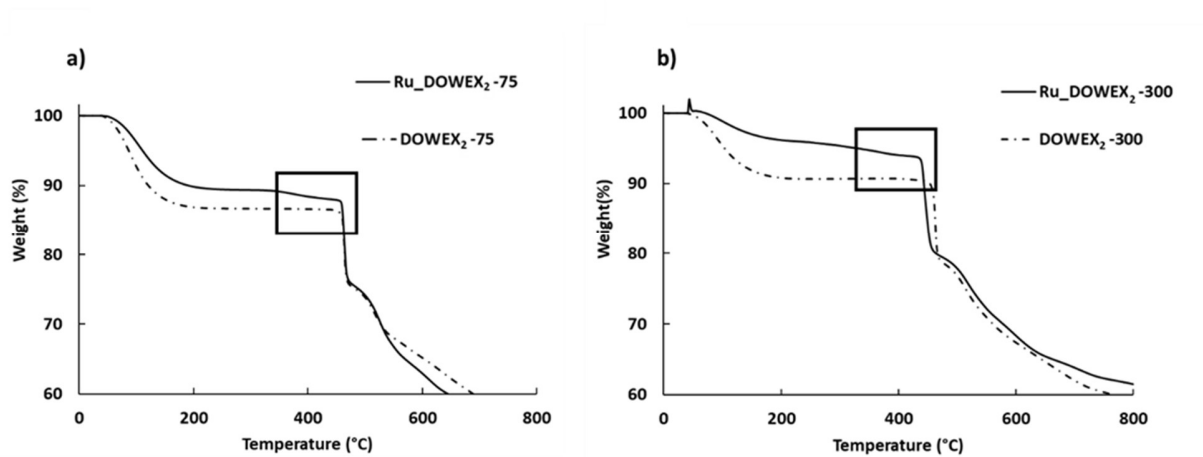


**Figure 1.** Thermograms of DOWEX<sub>2</sub>-X and Ru\_DOWEX<sub>2</sub>-X ((a): X=75; (b): X=300) under nitrogen atmosphere.

In order to get information on the existence, the shape, the size and the dispersion of the synthesized ruthenium NPs, transmission electron microscopy has been carried out (**Figure 2**). The TEM images confirm the existence of well-dispersed ruthenium particles with an average size of  $2.71 \pm 0.92$  nm and  $4.20 \pm 1.61$  nm for Ru\_DOWEX<sub>2</sub>-75 and Ru\_DOWEX<sub>2</sub>-300 respectively. The interaction of the ruthenium chloride with the sulfonate groups of the resin could provide more nucleation centers in order to get small ruthenium NPs. According to TEM images, the difference of the nanoparticles average size (around 1.50 nm) between the two materials could be correlated to the size of the bead acting as support (61 vs 250  $\mu$ m for DOWEX<sub>2</sub>-75 and DOWEX<sub>2</sub>-300 respectively). Moreover, using these TEM data, the ruthenium dispersion, which can be defined as the fraction of ruthenium atoms exposed to the surface, was estimated at 27% and 41% for Ru\_DOWEX<sub>2</sub>-75 and Ru\_DOWEX<sub>2</sub>-300 respectively (**ESI-pS6**).<sup>42</sup>

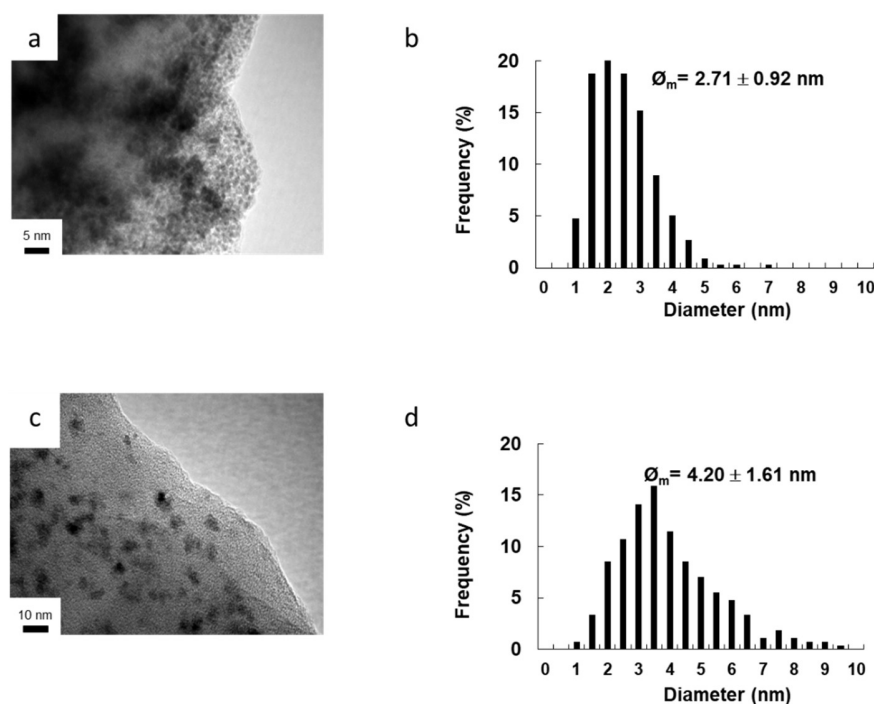


**Figure 2.** Transmission electron micrograph at a magnification of  $\times 200000$  and corresponding size distribution of Ru\_DOWEX<sub>2</sub>-75 (a, b) and Ru\_DOWEX<sub>2</sub>-300 (c, d).

## 2. Hydrogenation of methyl undecenoate as model reaction

The hydrogenation of vegetable oils derived compounds with resin-supported metal catalyst requires a good solvent combination. The first solvent is used for the resin swelling and the second one for the solubilization of the reactants but also the products in order to get a good reaction monitoring. One key parameter of resin-supported metal catalysts is the resin swelling, which will have an influence on the substrate proximity towards the catalytically metal particles in the DOWEX resins.<sup>36</sup> According to the literature data, the most efficient swelling solvents for gel-type resins are water and ethanol.<sup>39</sup> The C=C hydrogenation of methyl undecenoate, which was chosen as model substrate, was carried out at 30 °C, under 10 bar of hydrogen with a substrate/metal ratio of 180 in the presence of Ru\_DOWEX<sub>2</sub>-X (X=75 and 300) in heptane, an alkane-based solvent, with

a resin swelling solvent. We have tried ethanol/heptane and water/heptane combinations and compare the corresponding catalytic activities. The initial activity was higher than with water but, during the catalytic course, the activity rapidly slowed down. We observed the resin beads retraction, probably due to the partial solubilization of ethanol in heptane. That's the reason why water was chosen for the rest of this study.

### Influence of the volume of water

Prior to the introduction of the heptane-based solution of methyl undecenoate and the hydrogen in the glass vessel for the catalytic test, the resins were swelled with a precise volume of water directly in the glass vessel during two minutes. This period corresponds to the required time for reaching the maximum displaced water volume. The optimal amount of water was determined by evaluating the catalytic activity of the two swollen Ru\_DOWEX<sub>2</sub>-X (X=75 and 300) (**Figure 3**).

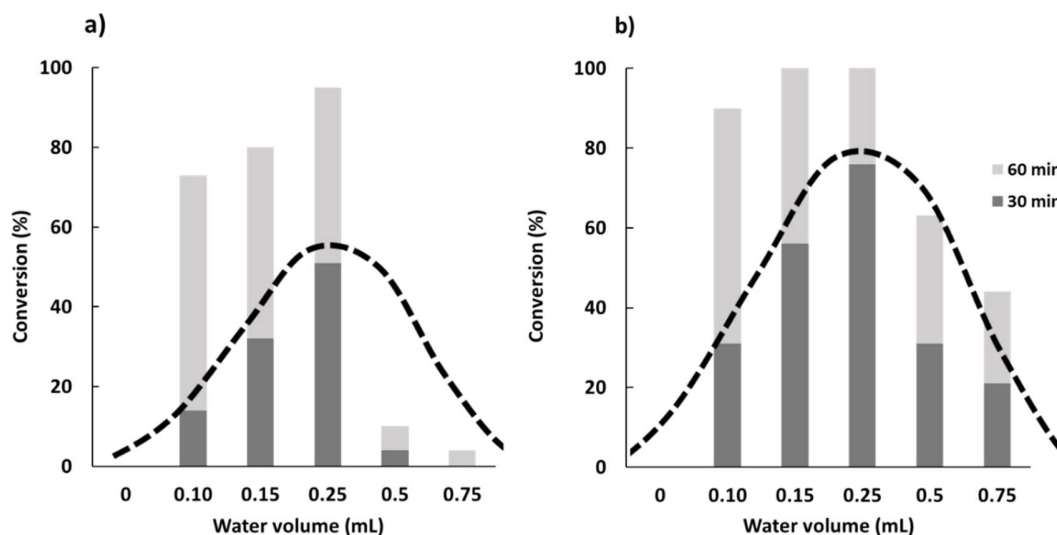


**Figure 3.** Influence of the water amount in DOWEX<sub>2</sub>-X-supported Ru NPs in the hydrogenation of methyl undecenoate ((a): Ru\_DOWEX<sub>2</sub>-75; (b): Ru\_DOWEX<sub>2</sub>-300).

Experimental conditions: Ru\_DOWEX<sub>2</sub>-X (100 mg, 8.9 μmol Ru), methyl undecenoate (316 mg, 1.60 mmol, 180 molar eq.), water (Y mL), heptane (6 mL), hydrogen pressure (10 bar), temperature (30° C), stirring rate (1000 rpm).

As it can be observed, whatever the beads size, a bell-shaped curve was obtained (**Figure 3**, dotted line) with an optimal conversion for a water volume of 0.25 mL. For lower water volumes, a catalytic activity drop was observed and could be explained by the partial swelling of the resin that reduced the active sites accessibility. On the other side, an excess of water involved a phase transfer step that slowed down the reaction rate. Whatever the water amount, the best catalytic activity was obtained for Ru\_DOWEX<sub>2</sub>-300. Its higher catalyst activity was not due to the size of the Ru NPs ( $4.20 \pm 1.61$  nm) which was higher than Ru\_DOWEX<sub>2</sub>-75 ( $2.71 \pm 0.92$  nm). The better activity of Ru\_DOWEX<sub>2</sub>-300 could be explained by the better dispersion of the beads in heptane in comparison with Ru\_DOWEX<sub>2</sub>-75 where visual bead aggregation could be seen in the bottom of the reactor glass (**ESI-Figure S2**). Moreover, from a recovery point of view, the bigger beads are easier to separate from the reaction medium. For these reasons, Ru\_DOWEX<sub>2</sub>-300 will be further used for the rest of the study. Finally, the influence of the temperature and the hydrogen pressure on the catalytic activity of Ru\_DOWEX<sub>2</sub>-300 has briefly been studied (**ESI-Figure S3**). As expected, an increase of the pressure or the temperature led to an activity improvement and no catalyst deactivation during the catalytic run was observed.

### **Recycling experiments**

The recyclability of Ru\_DOWEX<sub>2</sub>-300 has been studied considering the same experimental conditions described above. After 30 minutes of reaction, the reaction was stopped, the organic

phase (methyl undecenoate and methyl undecanoate in heptane) was removed and the solid catalyst was isolated and washed several times with heptane without drying and water regeneration. Gas chromatography analyses of the organic phase were performed to check if the organic substrate is still present. A second run can start after the addition of a fresh methyl undecenoate solution in heptane (**Figure 4**).

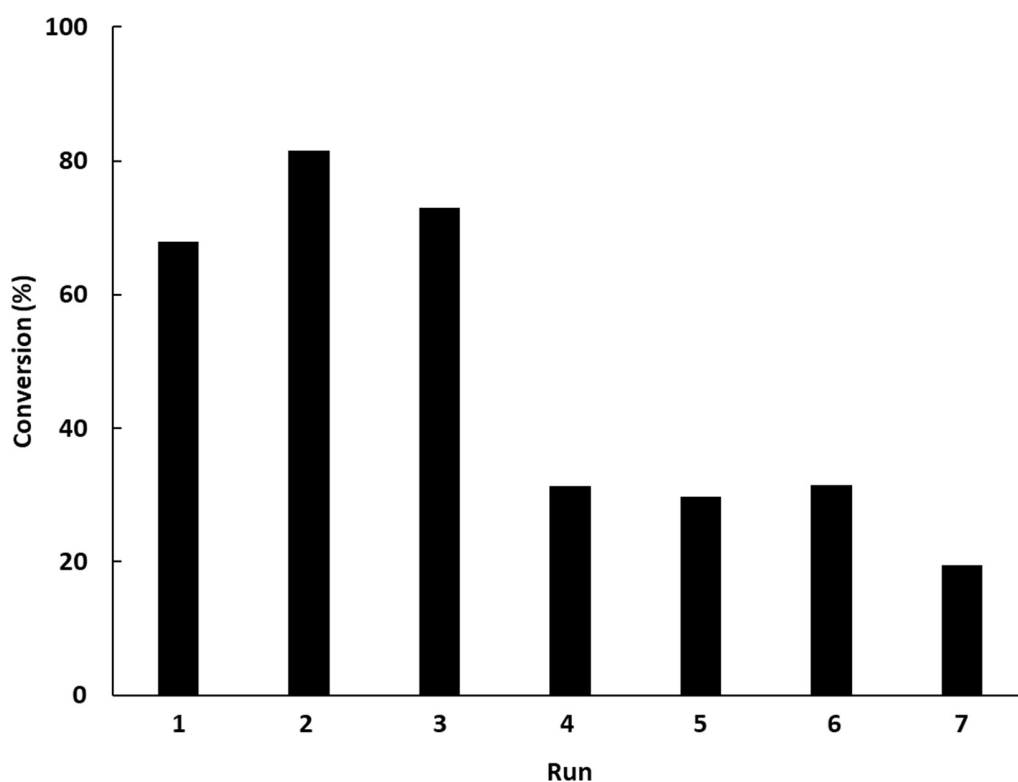


**Figure 4.** Recycling of Ru\_DOWEX<sub>2</sub>-300 in the hydrogenation of methyl undecenoate in heptane. Reaction Initial reaction conditions: Ru\_DOWEX<sub>2</sub>-300 (100 mg, 8.9  $\mu$ mol Ru), methyl undecenoate (361 mg, 1.6 mmol, 180 molar eq.), water (0.25 mL), heptane (6 mL), hydrogen pressure (10 bar), temperature (30 °C), stirring rate (1000 rpm), time (30 minutes).

According to **Figure 4**, the conversions for second and third runs are higher than that of the first run. This result could be explained by a catalyst pre-activation which occurred during the first run

with the hydrogen pressure to remove a possible oxide layer on ruthenium particles. It is important to precise that the resin-supported Ru NPs are not pre-reduced before the first run. It may also be possible that the optimal water volume is not exactly 0,25 mL. At the fourth run, a significant activity decrease was noticed (around 40 %) but kept constant during three consecutive runs. A new decrease was observed during the seventh run.

### **Limitations**

Several parameters could explain the above results such as *i*) an active phase degradation by a ruthenium leaching or an agglomeration of the metal nanoparticles, *ii*) a resin degradation due to the stirring but also *iii*) a loss of water inside the resin pores. In order to better understand our catalytic system, we performed several experiments to find the key parameters which strongly influence the activity of the catalytic system.

#### ***Active phase degradation***

A catalytic activity decrease with supported metallic nanoparticles is generally due to the loss of metal during the catalytic test or the agglomeration of the corresponding particles on the support.<sup>43,44</sup> We first checked if any ruthenium leaching occurred during a catalytic run through complementary experiments. After 30 minutes of reaction and removal of the metal catalyst from the glass vessel, the organic phase (methyl undecenoate and methyl undecanoate in heptane) was stirred under hydrogenation conditions for 18h (30 °C under 10 bar of hydrogen) and no activity was observed. Moreover, according to ICP analyses, less than 2 ppm of ruthenium were measured in the organic phase and no substantial metal loss in the ion-exchange resin has been observed

after several runs (8% of metal loss between the fresh catalyst and the catalyst after the 7th run). This dramatic activity decrease cannot be attributed to this metal loss.

TEM experiments were also performed to check the stability of the ruthenium nanoparticles in/on the support (**Figure 5**).

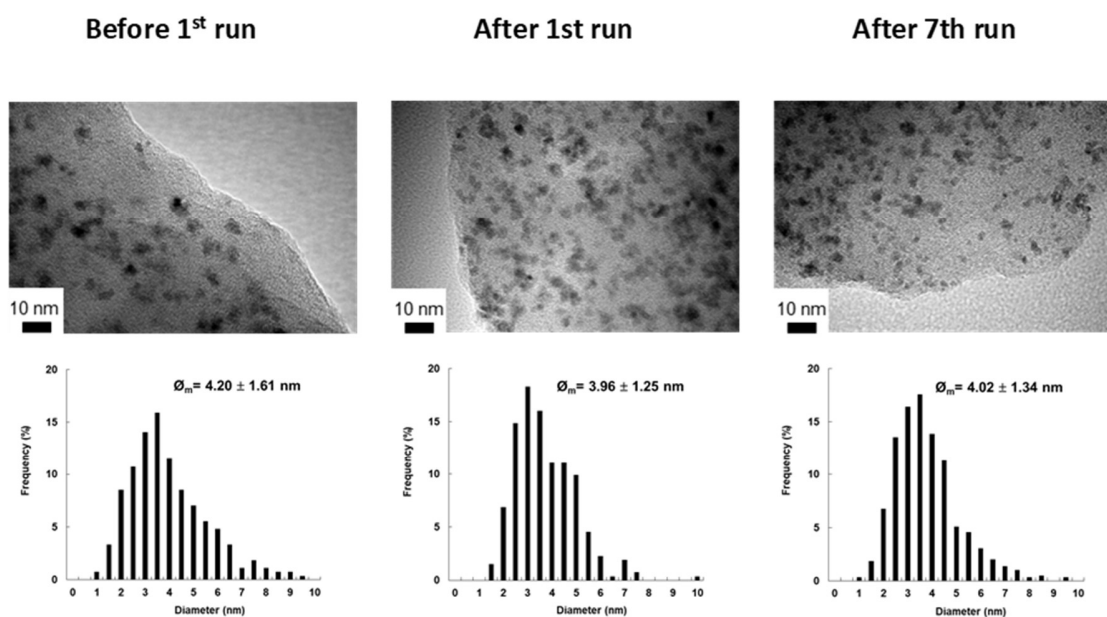


**Figure 5.** TEM images at a magnification of  $\times 200000$  and corresponding size distribution of Ru\_DOWEX<sub>2</sub>-300 after several runs of the catalytic hydrogenation of methyl undecenoate in heptane. Initial reaction conditions: Ru\_DOWEX<sub>2</sub>-300 (100 mg, 8.9  $\mu$ mol Ru), methyl undecenoate (361 mg, 1.6 mmol, 180 molar eq.), water (0.25 mL), heptane (6 mL), hydrogen pressure (10 bar), temperature (30° C), reaction time (30 min), stirring rate (1000 rpm).

According to the TEM images, neither particles aggregation nor change of the mean diameter size of the Ru NPs after several runs were observed. It can be concluded that the material showed a high robustness after seven catalytic runs and that the activity decrease did not come from the active phase particles degradation.

## *Mechanical damage*

Resin damages by stirring are possible during the catalytic tests. SEM experiments of the metal catalyst in dried state were carried out before the catalytic test and after the first and the seventh run (Figure 6).

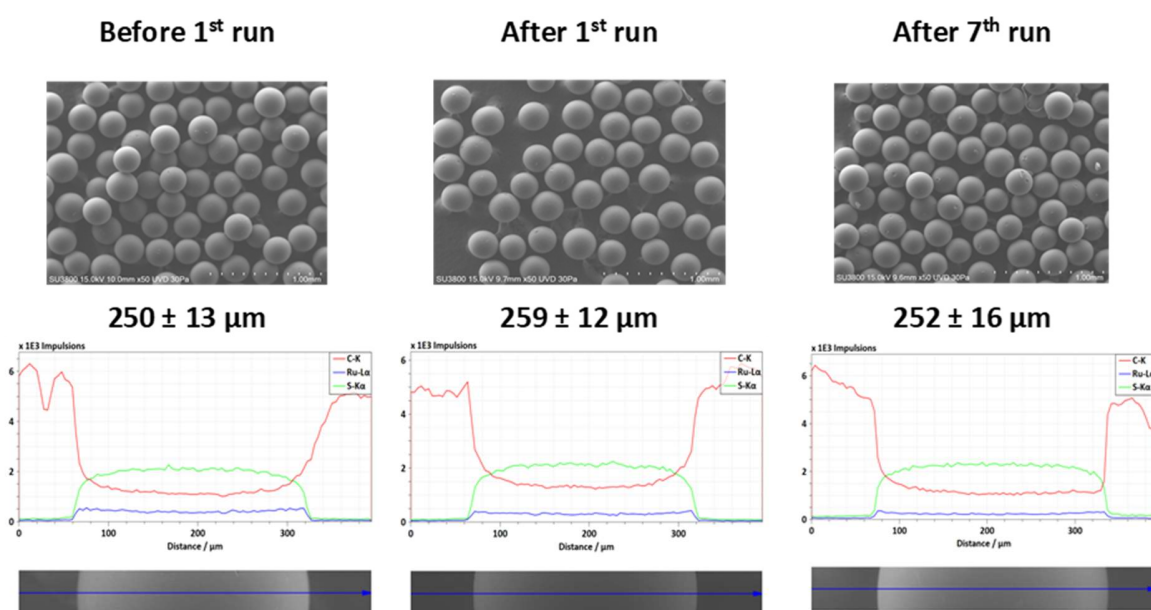


**Figure 6.** Scattering micrographs and corresponding ruthenium distribution along a traverse line across an equatorial section of a bead of Ru\_DOWEX<sub>2</sub>-300 after several runs of the catalytic hydrogenation of methyl undecenoate in heptane.

According to SEM images, no visual mechanical damages were observed during seven runs and the bead mean size kept constant. Moreover, according to EDS analyses, the ruthenium distribution

was also stable. These SEM images with the EDS ruthenium profile showed once again the robustness of the metal catalyst.

### *Water loss*

It was previously proven that the water amount inside the pores strongly influenced the catalytic activity and that too much or too less water led to a dramatic decrease in activity (**Figure 4**). Complementary experiments were performed to point out the importance of water inside the porous structure of the resin. The evolution of the bead size during the recycling study was evaluated through optic microscopy (**Figure 7**).

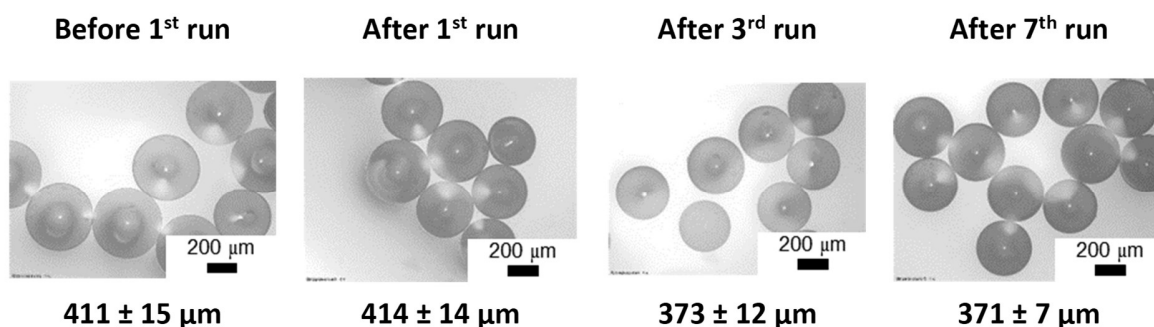


**Figure 7.** Evolution of the mean bead diameter of Ru\_DOWEX<sub>2</sub>-300 through optical microscopy (counting of 10-20 beads between each run) after several runs of the catalytic hydrogenation of methyl undecenoate

According to the images, a size decrease was measured from the third catalytic run. These observations are in good correlation with the catalytic activity decrease. In order to confirm that the bead size decrease came from the loss of water, after the seventh catalytic run, the catalyst was isolated, washed and dried at 60°C during 24 hours. A new catalytic run (called “7+1” run) could start after the addition of 0.25 mL of water (**ESI Figure S4**). The catalytic activity has improved

and reached a value close to the three first runs and this activity kept constant for the following run called “7+2”. The complete isolation of Ru\_DOWEX<sub>2</sub>-300 suggested that the catalytic system has lost water during the consecutive runs but could keep efficient through a strict control of the recycling procedure.

We decided to study the influence of the catalyst drying time on its activity (**ESI-Figure S5**). Taking into account the dramatic activity decrease from the fourth run (**Figure 4**), the water addition is performed after every three runs. For the first twelve runs, the catalyst was isolated every three runs and dried 48 hours at 60°C and a significative activity decrease was observed. After the twelfth run, the drying time was extended to 72 hours and a notable activity increase was observed, confirming that the drying time is a key parameter. After the fifteenth run, the time was shortened to 48 hours again and the catalytic activity was lower again.

A new recycling procedure has been performed in order to confirm the above hypothesis by setting the solid catalyst drying time at 72h (**Figure 8**).

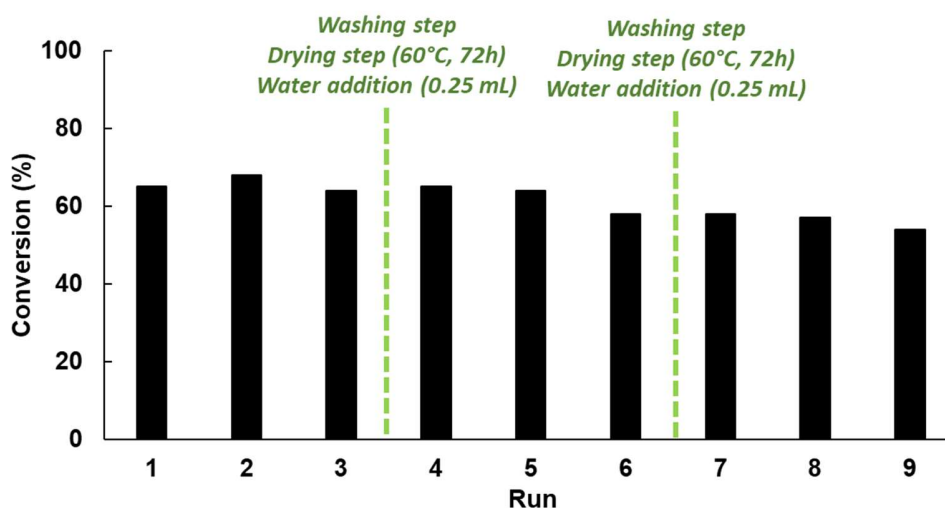


**Figure 8.** Recycling of Ru\_DOWEX<sub>2</sub>-300 in the hydrogenation of methyl undecenoate in heptane. Initial reaction conditions: Ru\_DOWEX<sub>2</sub>-300 (100 mg, 8.9  $\mu$ mol Ru), methyl undecenoate (361 mg, 1.6 mmol, 180 molar eq.), water (0.25 mL), heptane (6 mL), hydrogen pressure (10 bar), temperature (30 °C), stirring rate (1000 rpm), time (30 minutes). These reaction conditions are applied after the third and sixth runs with a washing and a drying step of the solid catalyst, followed by addition of water. For the others runs, no drying step and no water addition.

According to these recycling results, the isolation of the catalyst, especially the drying step was necessary to keep a catalytic activity close to the initial one. A slow activity decrease was however observed, which could be explained by the metal loss which was measured in the first recycling procedure (8 wt% of metal loss after seven runs).

Complementary experiments have been carried out to support this hypothesis by changing heptane with ethyl acetate with an optimal water volume for the Ru\_DOWEX<sub>2</sub>-300 swelling of 0.1 mL (**ESI-Figure S6**). The recycling was then performed under the same reaction conditions (**Figure 9**).

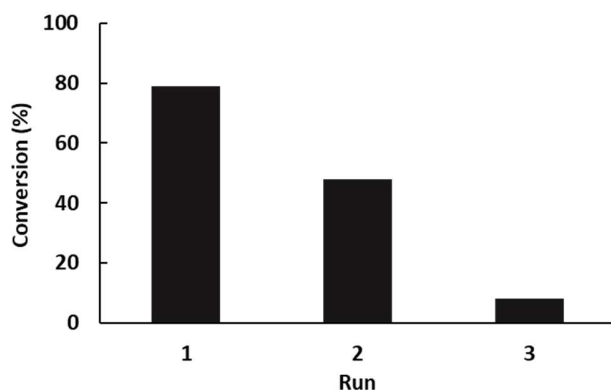


**Figure 9.** Recycling of Ru\_DOWEX<sub>2</sub>-300 in the hydrogenation of methyl undecenoate in ethyl acetate. Initial reaction conditions: Ru\_DOWEX<sub>2</sub>-300 (100 mg, 8.9  $\mu$ mol Ru), methyl undecenoate (316 mg, 1.6

mmol), water (0.1 mL), ethyl acetate (6 mL), hydrogen pressure (10 bar), temperature (30 °C), time (30 min), stirring rate (1000 rpm).

As it can be observed in Figure 4, the catalytic activity dropped to an activity close to zero after the 3<sup>rd</sup> run. Given that water is slightly soluble in ethyl acetate (8% wt), the resin swelling was no more optimal, leading to a lower availability of the Ru NPs. These recycling results confirmed our hypothesis concerning the correlation between the water amount inside the resin and the catalytic activity.

### 3. Hydrogenation of vegetable oils and their corresponding FAMES

The evaluation of the efficiency of Ru\_DOWEX<sub>2</sub>-300 was further extended in the hydrogenation of several fatty acid methyl esters (**Figure 10**).

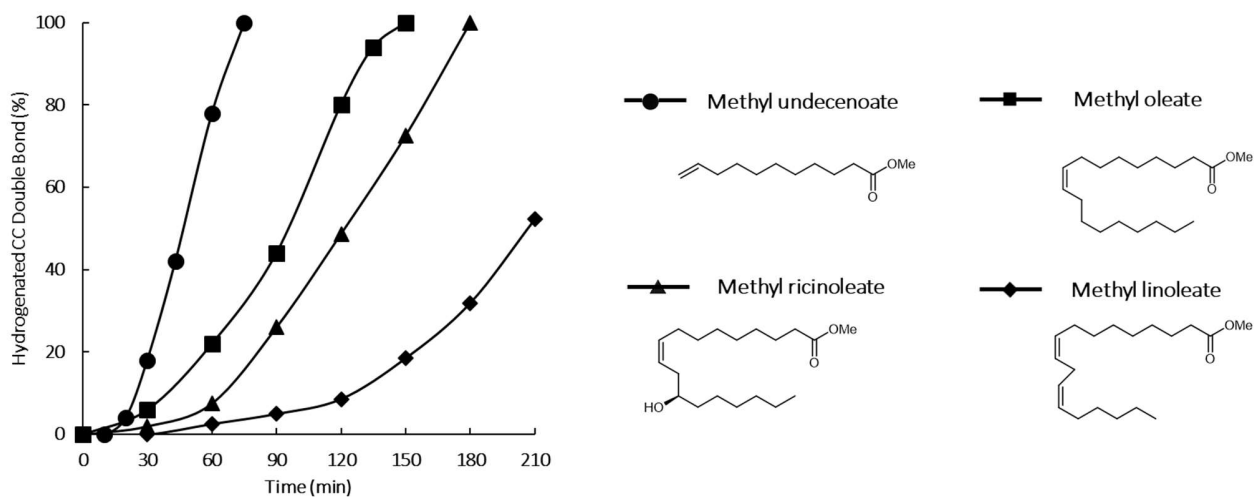


**Figure 10.** Catalytic hydrogenation of fatty acid methyl esters in the presence of DOWEX<sub>2</sub>-300-supported Ru NPs. Experimental conditions: Ru\_DOWEX<sub>2</sub>-300 (100 mg, 8.9  $\mu$ mol), substrate (1.6 mmol of double bond, 180 molar eq.), water (0.25 mL), heptane (6 mL), hydrogen pressure (10 bar), temperature (30 °C), stirring rate (1000 rpm).

According to the kinetic curves, the catalytic activity of the resin-supported Ru NPs depended firstly on the carbon chain length. Thus, the best activity was obtained with the C<sub>11</sub>-unsaturated ester, which has the shortest chain length in comparison with the three others C<sub>18</sub>-unsaturated esters. This trend has already been observed in biphasic catalysis with water soluble organometallic complexes. Moreover, the double bond is internal for these three C<sub>18</sub>-esters, slowing down the catalytic activity which has been obtained in a previous study.<sup>24</sup> The catalytic activity of the resin-supported Ru NPs depended also of the substrate hydrophobicity. Methyl ricinoleate, which is less hydrophobic due to the presence of a hydroxyl group, showed a lower reactivity in comparison with methyl oleate. A last point is the importance of the number of unsaturations. The reaction rate was strongly reduced in the case of the di-unsaturated methyl linoleate. This result could be explained by the lower linoleate concentration (twice less than oleate concentration).

We also evaluated the reactivity of the resin-supported Ru NPs towards the hydrogenation of vegetable oils-based compounds (**Figure 11**).

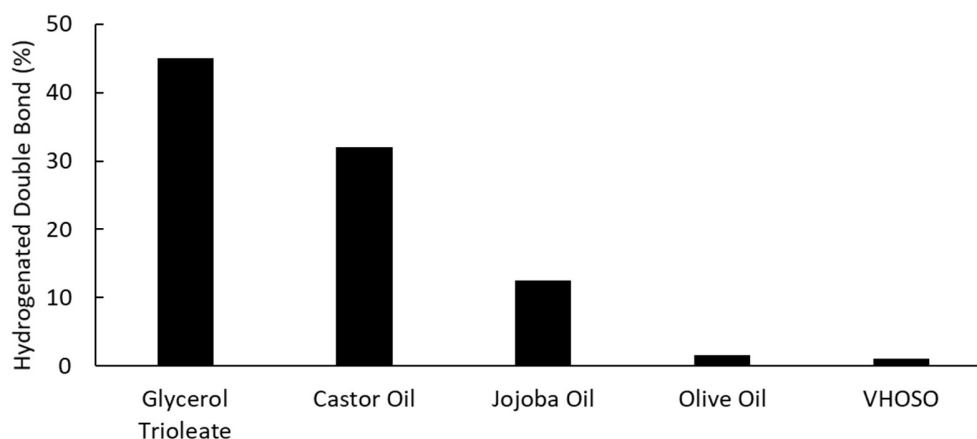


**Figure 11.** Catalytic hydrogenation of vegetable oils-based compounds in the presence of DOWEX<sub>2</sub>-300-supported Ru NPs. Experimental conditions: Ru\_ DOWEX<sub>2</sub>-300 (100 mg, 8.9 μmol), substrate (1.60 mmol of double bond, 180 molar eq.), water (0.25 mL), heptane (6 mL), hydrogen pressure (10 bar), temperature (30° C), reaction time (120 min), stirring rate (1000 rpm).

Glycerol trioleate and castor oil were converted in the presence of the resin-supported ruthenium NPs under mild experimental conditions (10 bar H<sub>2</sub>, 30 °C). A similar trend was observed where glycerol trioleate and castor oil were the most reactive substrates, like in the case of the corresponding FAMES (methyl oleate and ricinoleate respectively). Interestingly, in terms of hydrogenated double bond, the catalytic activity of Ru\_ DOWEX<sub>2</sub>-300 for the triglyceride (glycerol trioleate or castor oil) is close to their corresponding FAMES in spite of the oil chemical size. Jojoba oil, a di-unsaturated compound which is a mixture of eicosenoic (C<sub>20:1</sub>, 77%), erucic (C<sub>22:1</sub>, 12%) and oleic (C<sub>18:1</sub>, 10%) monoesters, has also been tested. The much lower conversion of Jojoba in comparison with the previous triglycerides could be explained by the higher carbon chain lengths.

It was also observed that the catalyst activity strongly depended of the presence of dienes in vegetable oils. For the olive oil and the VHOSO (very high-oleic sunflower oil), which contained around 5% of dienes, the catalytic activity dropped. This hypothesis could explain the previous methyl linoleate result (**Figure 10**) where isomerization could occur during the catalytic test.<sup>22,45,46</sup>

## Conclusions

Ion-exchange resin-supported ruthenium nanoparticles have been synthesized through a simple and efficient two-step procedure with no resin damages. According to all catalytic results, the Ru\_

DOWEX<sub>2</sub>-X activity strongly depended on the water amount inside the pores of the resin. Several controls were performed and showed a high robustness of the heterogeneous catalyst. Nevertheless, a bead mean size decrease, observed through optic and scattering electron microscopies, clearly showed that this activity decrease was due to the loss of water. The catalyst recycling, through a strict control of the procedure, confirmed the above comment. The remarkable catalytic activities towards C18-based unsaturated compounds, coupled with the easy recovery of a cheap support-based metal catalyst, emphasized the interest of this present catalytic system for the hydrogenation of vegetable oils derivatives in comparison with other ruthenium-supported catalysts.<sup>23,47</sup>

### **Supporting Information**

Experimental section (general information, preparation and characterization of the catalysts, catalytic test description); scanning electron microscopy experiments; recycling experiments; catalytic tests performed in ethyl acetate.

### **Corresponding Author**

\*Sébastien Noël - Univ. Artois, CNRS, Centrale Lille, Univ. Lille, UMR 8181, Unité de Catalyse et Chimie du Solide (UCCS), 62300 Lens, France. E-mail: [sebastien.noel@univ-artois.fr](mailto:sebastien.noel@univ-artois.fr)

### **Author Contributions**

The manuscript was written through contributions of all authors. All authors have given approval to the final version of the manuscript.

## Acknowledgments

The University of Artois and the region “Hauts-de-France” are acknowledged for funding this work. For the TEM analyses, the Chevreul Institute is thanked for its help in the development of this work through the ARCHI-CM project supported by the “Ministère de l’Enseignement Supérieur de la Recherche et de l’Innovation”, the Region “Hauts-de-France”, the ERDF program of the European Union and the “Métropole Européenne de Lille”. We are grateful to Ahmed Addad for TEM analyses. We thank Pr. Jean François Blach for optical microscopy analyses, Dr. Michel Ferreira for ICP analyses, Dr. Nicolas Kania, Dr. Jérémy Ternel and Dominique Prevost for technical assistance.

## References

- (1) Corma, A.; Iborra, S.; Velty, A. Chemical Routes for the Transformation of Biomass into Chemicals. *Chem. Rev.* **2007**, *107* (6), 2411–2502.
- (2) Margarida Martins, M.; Carvalheiro, F.; Gírio, F. An Overview of Lignin Pathways of Valorization: From Isolation to Refining and Conversion into Value-Added Products. *Biomass Convers. Biorefinery* **2022**. <https://doi.org/10.1007/s13399-022-02701-z>.
- (3) Zhou, C. H.; Xia, X.; Lin, C. X.; Tong, D. S.; Beltramini, J. Catalytic Conversion of Lignocellulosic Biomass to Fine Chemicals and Fuels. *Chem. Soc. Rev.* **2011**, *40* (11), 5588–5617. <https://doi.org/10.1039/c1cs15124j>.
- (4) Issariyakul, T.; Dalai, A. K. Biodiesel from Vegetable Oils. *Renew. Sustain. Energy Rev.* **2014**, *31*, 446–471. <https://doi.org/10.1016/j.rser.2013.11.001>.

- (5) Mishra, V. K.; Goswami, R. A Review of Production, Properties and Advantages of Biodiesel. *Biofuels* **2018**, *9* (2), 273–289. <https://doi.org/10.1080/17597269.2017.1336350>.
- (6) Brännström, H.; Kumar, H.; Alén, R. Current and Potential Biofuel Production from Plant Oils. *BioEnergy Res.* **2018**, *11* (3), 592–613. <https://doi.org/10.1007/s12155-018-9923-2>.
- (7) Kumar, D.; Kumar, A.; Singla, A.; Dewan, R. Production and Tribological Characterization of Castor Based Biodiesel. *Mater. Today Proc.* **2021**, *46*, 10942–10949. <https://doi.org/https://doi.org/10.1016/j.matpr.2021.02.009>.
- (8) Osorio-González, C. S.; Gómez-Falcon, N.; Sandoval-Salas, F.; Saini, R.; Brar, S. K.; Ramírez, A. A. Production of Biodiesel from Castor Oil: A Review. *Energies* . 2020. <https://doi.org/10.3390/en13102467>.
- (9) Zhou, Y.; Huang, Y.; Fang, Y.; Tan, T. Selective Conversion of Castor Oil Derived Ricinoleic Acid Methyl Ester into Jet Fuel. *Green Chem.* **2016**, *18* (19), 5180–5189. <https://doi.org/10.1039/C6GC00942E>.
- (10) Hu, C.; Creaser, D.; Siahrostami, S.; Ojagh, H.; Skoglundh, M. Catalytic Hydrogenation of C=C and C=O in Unsaturated Fatty Acid Methyl Esters. *Catal. Sci. Technol.* **2014**, 2427–2444. <https://doi.org/10.1039/c4cy00267a>.
- (11) Yao, X.; Strathmann, T. J.; Li, Y.; Cronmiller, L. E.; Ma, H.; Zhang, J. Catalytic Hydrothermal Deoxygenation of Lipids and Fatty Acids to Diesel-like Hydrocarbons: A Review. *Green Chem.* **2021**, *23* (3), 1114–1129. <https://doi.org/10.1039/D0GC03707A>.
- (12) Chikkali, S.; Mecking, S. Refining of Plant Oils to Chemicals by Olefin Metathesis. *Angew. Chemie Int. Ed.* **2012**, *51* (24), 5802–5808. <https://doi.org/10.1002/anie.201107645>.
- (13) Fernández, M. B.; Tonetto, G. M.; Crapiste, G. H.; Damiani, D. E. Revisiting the Hydrogenation of Sunflower Oil over a Ni Catalyst. *J. Food Eng.* **2007**, *82* (2), 199–208.

<https://doi.org/10.1016/j.jfoodeng.2007.02.010>.

- (14) Cepeda, E. A.; Calvo, B.; Sierra, I.; Iriarte-Velasco, U. Selective Hydrogenation of Sunflower Oil over Ni Catalysts. *Korean J. Chem. Eng.* **2016**, *33* (1), 80–89. <https://doi.org/10.1007/s11814-015-0095-x>.
- (15) Zaccheria, F.; Psaro, R.; Ravasio, N. Selective Hydrogenation of Alternative Oils: A Useful Tool for the Production of Biofuels. *Green Chem.* **2009**, *11* (4), 462–465. <https://doi.org/10.1039/B817625F>.
- (16) Ravasio, N.; Zaccheria, F.; Gargano, M.; Recchia, S.; Fusi, A.; Poli, N.; Psaro, R. Environmental Friendly Lubricants through Selective Hydrogenation of Rapeseed Oil over Supported Copper Catalysts. *Appl. Catal. A , Gen.* **2002**, *233*, 1–6.
- (17) Zhao, Y.; Ren, Y.; Zhang, R.; Zhang, L.; Yu, D.; Jiang, L.; Elfalleh, W. Preparation of Hydrogenated Soybean Oil of High Oleic Oil with Supported Catalysts. *Food Biosci.* **2018**, *22*, 91–98. <https://doi.org/https://doi.org/10.1016/j.fbio.2018.01.010>.
- (18) Chorfa, N.; Hamoudi, S.; Arul, J.; Belkacemi, K. Sulfur Promotion in Conjugated Isomerization of Safflower Oil over Bifunctional Structured Rh/SBA-15 Catalysts. *ChemCatChem* **2013**, *5* (7), 1917–1934. <https://doi.org/10.1002/cctc.201200895>.
- (19) Nohair, B.; Especel, C.; Lafaye, G.; Marécot, P.; Hoang, L. C.; Barbier, J. Palladium Supported Catalysts for the Selective Hydrogenation of Sunflower Oil. *J. Mol. Catal. A Chem.* **2005**, *229* (1), 117–126.
- (20) Quaranta, E.; Cornacchia, D. Partial Hydrogenation of a C18:3-Rich FAME Mixture over Pd/C. *Renew. Energy* **2020**, *157*, 33–42. <https://doi.org/https://doi.org/10.1016/j.renene.2020.04.122>.
- (21) Toshtay, K.; Auezov, A. B. Hydrogenation of Vegetable Oils over a Palladium Catalyst

- Supported on Activated Diatomite. *Catal. Ind.* **2020**, *12* (1), 7–15.  
<https://doi.org/10.1134/S2070050420010109>.
- (22) Bernas, A.; Murzin, D. Y. Linoleic Acid Isomerization on Ru/Al<sub>2</sub>O<sub>3</sub> Catalyst: 1: Conjugation and Hydrogenation. *Chem. Eng. J.* **2005**, *115* (1), 13–22.  
<https://doi.org/https://doi.org/10.1016/j.cej.2005.09.001>.
- (23) Mäki-Arvela, P.; Kuusisto, J.; Sevilla, E. M.; Simakova, I.; Mikkola, J.-P.; Myllyoja, J.; Salmi, T.; Murzin, D. Y. Catalytic Hydrogenation of Linoleic Acid to Stearic Acid over Different Pd- and Ru-Supported Catalysts. *Appl. Catal. A Gen.* **2008**, *345* (2), 201–212.
- (24) Noël, S.; Madureira, A.; Léger, B.; Ponchel, A.; Sadjadi, S.; Monflier, É. Cyclodextrin-Assisted Catalytic Hydrogenation of Hydrophobic Substrates with Halloysite Immobilized Ruthenium NPs Dispersed in Aqueous Phase. *J. Indian Chem. Soc.* **2021**, *98* (3), 100034.  
<https://doi.org/https://doi.org/10.1016/j.jics.2021.100034>.
- (25) Troncoso, F. D.; Tonetto, G. M. Highly Stable Platinum Monolith Catalyst for the Hydrogenation of Vegetable Oil. *Chem. Eng. Process. - Process Intensif.* **2022**, *170*, 108669. <https://doi.org/https://doi.org/10.1016/j.cep.2021.108669>.
- (26) Iida, H.; Itoh, D.; Minowa, S.; Yanagisawa, A.; Igarashi, A. Hydrogenation of Soybean Oil over Various Platinum Catalysts: Effects of Support Materials on Trans Fatty Acid Levels. *Catal. Commun.* **2015**, *62*, 1–5. <https://doi.org/10.1016/j.catcom.2014.12.025>.
- (27) Laverdura, U. P.; Rossi, L.; Ferella, F.; Courson, C.; Zarli, A.; Alhajjoussef, R.; Gallucci, K. Selective Catalytic Hydrogenation of Vegetable Oils on Lindlar Catalyst. *ACS Omega* **2020**, *5* (36), 22901–22913. <https://doi.org/10.1021/acsomega.0c02280>.
- (28) Barbaro, P.; Liguori, F. Ion Exchange Resins: Catalyst Recovery and Recycle. *Chem. Rev.* **2009**, *109* (2), 515–529. <https://doi.org/10.1021/cr800404j>.

- (29) Liguori, F.; Moreno-Marrodan, C.; Barbaro, P. Metal Nanoparticles Immobilized on Ion-Exchange Resins: A Versatile and Effective Catalyst Platform for Sustainable Chemistry. *Chinese J. Catal.* **2015**, *36* (8), 1157–1169. [https://doi.org/https://doi.org/10.1016/S1872-2067\(15\)60865-8](https://doi.org/https://doi.org/10.1016/S1872-2067(15)60865-8).
- (30) Corain, B.; Zecca, M.; Jeřábek, K. Catalysis and Polymer Networks — the Role of Morphology and Molecular Accessibility. *J. Mol. Catal. A Chem.* **2001**, *177* (1), 3–20. [https://doi.org/https://doi.org/10.1016/S1381-1169\(01\)00305-3](https://doi.org/https://doi.org/10.1016/S1381-1169(01)00305-3).
- (31) Biffis, A.; D'Archivio, A. A.; Jerábek, K.; Schmid, G.; Corain, B. The Generation of Size-Controlled Palladium Nanoclusters Inside Gel-Type Functional Resins: Arguments and Preliminary Results. *Adv. Mater.* **2000**, *12* (24), 1909–1912. [https://doi.org/https://doi.org/10.1002/1521-4095\(200012\)12:24<1909::AID-ADMA1909>3.0.CO;2-4](https://doi.org/https://doi.org/10.1002/1521-4095(200012)12:24<1909::AID-ADMA1909>3.0.CO;2-4).
- (32) Bradu, C.; Căpăț, C.; Papa, F.; Frunza, L.; Olaru, E.-A.; Crini, G.; Morin-Crini, N.; Euvrard, É.; Balint, I.; Zgura, I.; Munteanu, C. Pd-Cu Catalysts Supported on Anion Exchange Resin for the Simultaneous Catalytic Reduction of Nitrate Ions and Reductive Dehalogenation of Organochlorinated Pollutants from Water. *Appl. Catal. A Gen.* **2019**, *570*, 120–129. <https://doi.org/https://doi.org/10.1016/j.apcata.2018.11.002>.
- (33) Sánchez, B. S.; Gross, M. S.; Querini, C. A. Pt Catalysts Supported on Ion Exchange Resins for Selective Glycerol Oxidation. Effect of Au Incorporation. *Catal. Today* **2017**, *296*, 35–42. <https://doi.org/https://doi.org/10.1016/j.cattod.2017.05.082>.
- (34) Liguori, F.; Barbaro, P.; Calisi, N. Continuous-Flow Oxidation of HMF to FDCA by Resin-Supported Platinum Catalysts in Neat Water. *ChemSusChem* **2019**, *12* (12), 2558–2563. <https://doi.org/https://doi.org/10.1002/cssc.201900833>.

- (35) Seki, T.; Grunwaldt, J.-D.; van Vegten, N.; Baiker, A. Palladium Supported on an Acidic Resin: A Unique Bifunctional Catalyst for the Continuous Catalytic Hydrogenation of Organic Compounds in Supercritical Carbon Dioxide. *Adv. Synth. Catal.* **2008**, *350* (5), 691–705. <https://doi.org/https://doi.org/10.1002/adsc.200700532>.
- (36) Marrodan, C. M.; Berti, D.; Liguori, F.; Barbaro, P. In Situ Generation of Resin-Supported Pd Nanoparticles under Mild Catalytic Conditions: A Green Route to Highly Efficient, Reusable Hydrogenation Catalysts. *Catal. Sci. Technol.* **2012**, *2* (11), 2279–2290. <https://doi.org/10.1039/C2CY20205K>.
- (37) Moreno-Marrodan, C.; Liguori, F.; Mercadé, E.; Godard, C.; Claver, C.; Barbaro, P. A Mild Route to Solid-Supported Rhodium Nanoparticle Catalysts and Their Application to the Selective Hydrogenation Reaction of Substituted Arenes. *Catal. Sci. Technol.* **2015**, *5* (7), 3762–3772. <https://doi.org/10.1039/C5CY00599J>.
- (38) Moreno-Marrodan, C.; Barbaro, P. Energy Efficient Continuous Production of  $\gamma$ -Valerolactone by Bifunctional Metal/Acid Catalysis in One Pot. *Green Chem.* **2014**, *16* (7), 3434–3438. <https://doi.org/10.1039/C4GC00298A>.
- (39) Ramírez, E.; Bringué, R.; Fité, C.; Iborra, M.; Tejero, J.; Cunill, F. Assessment of Ion Exchange Resins as Catalysts for the Direct Transformation of Fructose into Butyl Levulinate. *Appl. Catal. A Gen.* **2021**, *612*, 117988. <https://doi.org/https://doi.org/10.1016/j.apcata.2021.117988>.
- (40) Barbaro, P.; Bianchini, C.; Giambastiani, G.; Oberhauser, W.; Bonzi, L. M.; Rossi, F.; Dal Santo, V. Recycling Asymmetric Hydrogenation Catalysts by Their Immobilisation onto Ion-Exchange Resins. *Dalt. Trans.* **2004**, No. 12, 1783–1784. <https://doi.org/10.1039/B406179A>.

- (41) Karmore, V.; Madras, G. Thermal Degradation of Polystyrene by Lewis Acids in Solution. *Ind. Eng. Chem. Res.* **2002**, *41* (4), 657–660. <https://doi.org/10.1021/ie0104262>.
- (42) Johnston, R. L. *Atomic and Molecular Clusters*, 1st Editio.; CRC Press: London, 2002. <https://doi.org/https://doi.org/10.1201/9780367805814>.
- (43) Yang, W.; Vogler, B.; Lei, Y.; Wu, T. Metallic Ion Leaching from Heterogeneous Catalysts: An Overlooked Effect in the Study of Catalytic Ozonation Processes. *Environ. Sci. Water Res. Technol.* **2017**, *3* (6), 1143–1151. <https://doi.org/10.1039/C7EW00273D>.
- (44) Maillard, F.; Schreier, S.; Hanzlik, M.; Savinova, E. R.; Weinkauf, S.; Stimming, U. Influence of Particle Agglomeration on the Catalytic Activity of Carbon-Supported Pt Nanoparticles in CO Monolayer Oxidation. *Phys. Chem. Chem. Phys.* **2005**, *7* (2), 385–393. <https://doi.org/10.1039/B411377B>.
- (45) Philippaerts, A.; Goossens, S.; Jacobs, P. A.; Sels, B. F. Catalytic Production of Conjugated Fatty Acids and Oils. **2011**, 684–702. <https://doi.org/10.1002/cssc.201100086>.
- (46) Philippaerts, A.; Goossens, S.; Vermandel, W.; Tromp, M.; Turner, S. Design of Ru – Zeolites for Hydrogen-Free Production of Conjugated Linoleic Acids. **2011**, 757–767. <https://doi.org/10.1002/cssc.201100015>.
- (47) Xu, B.; Liew, K. Y.; Li, J. Effect of Ru Nanoparticle Size on Hydrogenation of Soybean Oil. *JAACS, J. Am. Oil Chem. Soc.* **2007**, *84* (2), 117–122. <https://doi.org/10.1007/s11746-006-1014-4>.